Research Square

Preprints are preliminary reports that have not undergone peer review.
They should not be considered conclusive, used to inform clinical practice,
or referenced by the media as validated information.

Closed-loop EEG feedback pacing regulates task load during digital learning

Katrina Sollazzo

katrina.sollazzo@hec.ca

HEC Montréal

Alexander John Karran
HEC Montréal

Thaddé Rolon-Merette
HEC Montréal

Alejandra Ruiz-Segura
HEC Montréal

Constantinos K. Coursaris
HEC Montréal

Pierre-Majorique Léger
HEC Montréal

Sylvain Sénécal
HEC Montréal

Article

Keywords:

Posted Date: July 14th, 2026

DOI: https://doi.org/10.21203/rs.3.rs-10167580/v1

License: This work is licensed under a Creative Commons Attribution 4.0 International License.
Read Full License

Additional Declarations: No competing interests reported.

Version of Record: A version of this preprint was published at Scientific Reports on October 21st, 2026.
See the published version at https://doi.org/10.1038/s41598-026-76321-2.

Abstract

Digital learning systems rarely adapt to momentary cognitive state, creating risk of underload or overload. The current study testes whether EEG-based closed-loop pacing can regulate task load dynamics during a digital constellation-learning task. Fifty-one participants were randomly assigned to adaptive, reward, or control conditions. In the adaptive condition, a task loas index derived from frontal theta and parietal alpha adjusted feedback duration between 3 and 8 s; fixed 5s feedback was used in reward and control conditions, with reward participants receiving performance-contingent draw entries. Accuracy increased across blocks in all groups, with no significant group or group-by-block effect. In contrast, EEG indices showed group-specific trajectories: task load decreased over time in the adaptive condition, and frontal theta and parietal alpha showed significant group-by-block interactions. The adaptive condition also showed reduced ate-session feedback duration, while reward participants reported higher satisfaction. intrinsic motivation did not moderate group effects, although perceived competence predicated final-block performance and interest and effort predicted engagement. These findings suggest that EEG-based feedback pacing can regulate neurophysiological task load dynamics despite lack of immediate accuracy gains under the present task constraints. The results support neuroadaptive scaffolding as a state-regulation mechanism for digital learning.

Introduction

Learning is a fundamental mechanism of human cognitive development, enabling knowledge consolidation, skill acquisition, and adaptive responses to environmental demands. The capacity for continuous learning represents an important skill for both personal and professional growth. Contemporary education spans a wide range of modalities, from traditional classroom instruction to digitally mediated learning environments. Over the past decade, the expansion of online learning has transformed educational delivery across domains. Recent estimates indicate that approximately 30% of individuals in developed economies engaged with online educational content in 2023, with participation reaching 33% in the European Union in 2024, reflecting sustained year-on-year growth [1, 2]. This widespread adoption highlights the need for rigorous evaluation of digital learning systems' efficacy to ensure pedagogical objectives align with learner outcomes [3].

A central advantage of online learning environments lies in their potential for individualized instruction. Educational research consistently shows that tailoring instructional methods to learners’ needs enhances knowledge acquisition and retention [4, 5]. However, most current digital learning platforms lack the capacity to assess learners’ cognitive states in real-time. As a result, instructional demands may become misaligned with learners’ available cognitive resources, potentially leading to disengagement, inefficiency, or cognitive overload [6]. Addressing this limitation requires adaptive mechanisms that continuously monitor cognitive state and adjust instructional parameters accordingly.

Neuroadaptive systems offer a promising avenue for addressing cognitive misalignment in digital learning. Such systems rely on brain-computer interfaces (BCIs) that infer cognitive states from

neurophysiological signals and use these inferences to drive real-time system adaptations. Brain-computer interfaces can be broadly categorised into invasive systems using implanted electrodes [7], active systems that require volitional modulation of neural signals for explicit control [8], and passive systems that continuously monitor spontaneous neural activity; however, these categories are not mutually exclusive. Passive BCIs are particularly well-suited to educational contexts, given that they operate implicitly and do not require deliberate user control.

Passive neuroadaptive systems typically acquire neural signals using non-invasive modalities such as electroencephalography (EEG) or functional near-infrared spectroscopy (fNIRS) [9]. Classification algorithms decode neural oscillatory patterns or haemodynamic responses to infer cognitive states, including sustained attention [10], level of cognitive load [11], and mental fatigue [12]. These inferred states then drive interface adaptations via predefined rule-based mechanisms, forming a closed-loop biocybernetic system [13]. This closed loop biocybernetic architecture, in which neurophysiological signals are continuously transformed into adaptive system responses, is illustrated in Fig. 1. Passive BCIs have been successfully implemented in domains such as aviation workload management [14, 15], vehicular attention monitoring [16, 17], educational engagement management [18], frustration detection[19], time perception [20]. In educational contexts, these systems leverage neurophysiological correlates of learning processes, such as attentional focus [21], cognitive engagement [22] and learning speed [23].

The effectiveness of neuroadaptive educational systems depends fundamentally on two interdependent factors: the accuracy with which cognitive states are classified and the pedagogical validity of the adaptations they trigger. This dual dependence requires careful consideration of both the theoretical frameworks that guide adaptation strategies and the neurophysiological indices used to discriminate among cognitive states.

Pedagogical validity in neuroadaptive learning systems is grounded in established learning theory, particularly scaffolding principles derived from sociocultural Vygotskian perspectives [24]. Scaffolding aims to maintain learners within their zone of proximal development (ZPD), defined as the range of challenge in which learners can achieve competencies beyond their independent capabilities through appropriate instructional support [25]. Educational technologies are increasingly operationalising scaffolding through computational mechanisms, including intelligent tutoring systems that provide adaptive guidance [26].

Research across educational neuroscience, cognitive psychology, and human-computer interaction has identified multiple scaffolding modalities, including interface modification, parametric task adjustment, and instructional sequencing [27–29]. For neuroadaptive systems, establishing a clear causal relationship between neural state inference and learning outcomes requires adaptation mechanisms that map unambiguously onto a single cognitive dimension. Parametric task adjustment offers a particularly tractable approach in this regard.

One such implementation involves the temporal modulation of stimulus presentation [11], whereby presentation duration is dynamically adjusted in response to changes in inferred cognitive demand. This approach operationalises the principle that learning efficiency is maximised when instructional pacing aligns with learners' momentary processing capacity. Accelerating presentation under low demand prevents disengagement, whereas extending presentation under high demand alleviates overload. Temporal modulation, therefore, enables adaptive calibration of instructional pacing while preserving a unidimensional relationship between neural measurement and system response.

The effectiveness of adaptive scaffolding depends, fundamentally, on the selection of an appropriate cognitive construct to drive system adaptation. In the learning sciences, several related constructs are used to characterise cognitive demand, including cognitive load, mental workload, and task load. Cognitive load refers specifically to working memory demands associated with information encoding, storage, and manipulation [30, 31]. Mental workload encompasses both objective resource expenditure and subjective perceptions of task demand [32, 33]. Task load integrates these perspectives within a multidimensional framework, incorporating intrinsic, extraneous, germane, and sensorimotor components that arise from task complexity, environmental factors, and the requirements for mobilising cognitive resources [34].

In this study, task load is adopted as the primary operational construct for neuroadaptive control. Task load captures moment-to-moment fluctuations in cognitive resource utilisation during task execution and provides a stable foundation for instructional calibration. Insufficient task load is associated with disengagement through under-stimulation, whereas excessive task load leads to performance degradation and motivational decline [35]. Maintaining learners within an optimal range of task load, therefore, aligns closely with the ZPD and supports effective scaffolding.

Task load can be quantified using neurophysiological markers derived from electroencephalographic signals. Prior research indicates that frontal theta oscillations reliably index cognitive resource allocation, sustained attention, and working memory engagement [36–38]. Parietal alpha suppression has been associated with attentional allocation and cognitive fatigue [39–41]. A composite index integrating frontal theta enhancement and parietal alpha modulation may provide a practical and plausible representation of task load that can be used in passive BCIs. Discretising task load into low, medium, and high states aligns with theoretical distinctions between underload, optimal load, and overload, corresponding to regions below, within, and above the ZPD [24, 42]. Real-time classification of these states allows for ongoing system calibration to sustain the cognitive conditions that support learning.

While cognitive state regulation is necessary for effective neuroadaptive learning, learning outcomes are also shaped by motivational dynamics that influence how learners allocate cognitive resources. Motivation modulates effort investment under variable task demands and interacts with the mechanisms that govern cognitive load regulation. Integrating motivation into neuroadaptive learning models is therefore essential.

Research combining cognitive load and self-determination theories suggests that instructional adaptations supporting autonomy and competence can reduce extraneous cognitive load while sustaining intrinsic motivation [43, 44]. From a neuroeconomic perspective, the subjective cost of mental effort is weighed against anticipated rewards, such that motivation increases willingness to invest cognitive resources when perceived value is high [45]. Within this framework, task load functions as a regulatory control signal that constrains how motivational states translate into sustained effort.

Intrinsic and extrinsic motivation influence learning through partially distinct mechanisms. Intrinsic motivation boosts attentional engagement and reward-related processing, while extrinsic motivation aids learning by reducing distractions and enhancing goal-oriented control [46]. Neurophysiological evidence indicates that intrinsic motivation is associated with increased frontal midline theta activity and alpha desynchronization during demanding tasks without corresponding gains in objective accuracy [47]. Extrinsic motivation has been linked to modulations in alpha power and frontal theta activity in working memory contexts [48–50].

Motivational intensity theory further predicts that effort investment scales with perceived task demand [51]. Separating task load from experienced mental load allows the examination of how motivation governs effort allocation under controlled cognitive conditions. From an educational perspective, effective learning requires maintaining learners within an optimal range of challenge that promotes engagement without exceeding available resources, a range that closely corresponds to the ZPD.

Building on this theoretical and methodological foundation, the present study investigates whether task load-driven neuroadaptive scaffolding can enhance learning performance in a digital learning environment and how its effects compare to those of extrinsic motivation. We develop a digital learning interface that dynamically regulates the duration of stimulus presentation based on real-time classification of task load derived from electroencephalographic signals. Using a passive brain-computer interface, task load is inferred continuously and categorised into low, medium, and high states, which trigger adaptive adjustments to instructional pacing.

The present study tested whether closed-loop EEG-based feedback pacing regulates task-load dynamics during digital learning. The study employs a between-subjects design with three conditions: neuroadaptive scaffolding, extrinsic motivation, and control. Participants complete a multi-block constellation learning task. In the adaptive condition, presentation duration varies as a function of classified task load. In the extrinsic motivation condition, participants are informed that performance determines entry into a monetary reward draw. In the control condition, presentation duration remains fixed. We distinguished behavioural learning outcomes from neurophysiological state-regulation outcomes. The primary behavioural outcome was blockwise task accuracy. The primary state-regulation outcome was change in EEG-derived task load across learning blocks. We predicted that all participants would improve over time, but that neuroadaptive feedback pacing would produce a distinct task-load trajectory relative to fixed-feedback control and reward conditions. We further examined autonomic

physiology, satisfaction, intention to recommend, engagement, and intrinsic motivation as secondary or exploratory outcomes

Results

In accordance with the neuroadaptive framework, first the continuous EEG indices of task load were examined to assess whether there was different modulation of TL across groups and blocks. Subsequent sections detail the behavioural performance, peripheral physiology and subjective perceptions.

Impact on brain activity

Task Load Index

To examine whether task load changed over the course of the session, we tested linear block contrasts in the mixed-effects model (with Block 1 as the reference). Collapsed across groups, the mixed ANOVA revealed no significant main effect of block, $F(3, 99) = 0.32$, $p = .814$, $\eta^2p = .009$, indicating that task load did not decrease uniformly across all participants. However, block contrasts in the mixed-effects model showed significant reductions relative to Block 1 in later blocks (Block 2: $z = -0.34$, $p = .732$; Block 3: $z = -2.16$, $p = .031$; Block 4: $z = -3.32$, $p < .001$). Descriptive data indicated that this pattern was driven primarily by the Adaptive group, whose mean task load decreased from Block 1 ($M = 2.14$, $SD = 0.34$) to Block 4 ($M = 1.92$, $SD = 0.30$), whereas task load remained relatively stable in the Control (Block 1: $M = 1.31$, $SD = 0.31$; Block 4: $M = 1.43$, $SD = 0.44$) and Reward groups (Block 1: $M = 1.37$, $SD = 0.28$; Block 4: $M = 1.37$, $SD = 0.33$). The significant Group by Block interaction, $F(6, 99) = 3.62$, $p = .003$, $\eta^2p = .18$, indicated that the time course of task load differed across groups. Together, these results indicate that task load reduced over time in the Adaptive condition, but not in the fixed-feedback Control and Reward conditions.

Frontal theta and parietal alpha

To assess differences in frontal theta (ROI including F1, F2, F3 and F4) and parietal alpha (ROI including CP1, CP5, P1, P5) between groups across the learning progression, a 3 (Group: Adaptive, Control, Reward) × 4 (Block: 1, 2, 3, 4) Mixed ANOVA was conducted for both frontal theta and parietal alpha relative power. All post-hoc pairwise comparisons were corrected using the False Discovery Rate (FDR) method, see Table 1 and Table 2.

Table 1
Mixed ANOVA Results for Alpha and Theta band power

	ROI	F-value	p-FDR	η_p^2
Frontal Theta	Group	1.29	0.347	0.075
	Block	3.38	0.032	0.095
	Interaction	6.88	< .001	0.301
Parietal Alpha	Group	0.87	0.428	0.052
	Block	3.1	0.032	0.089
	Interaction	4.14	0.002	0.206

For frontal theta power, there was no significant main effect of Group, $F(2, 35) = 1.29$, $p = .347$, $\eta_p^2 = .075$. However, there was a significant main effect of Block, $F(3, 105) = 3.38$, $p = .032$, $\eta_p^2 = .095$. Crucially, this was qualified by a robust Group by Block interaction, $F(6, 105) = 6.88$, $p < .001$, $\eta_p^2 = .301$, indicating that frontal theta trajectories varied significantly by intervention (see Table 1 and Fig. 4). Post-hoc pairwise comparisons revealed that during the initial stages of learning, the Adaptive group exhibited higher frontal theta power compared to the Control group (Block 1: $p = .038$; Block 2: $p = .043$; Block 3: $p = .043$). The Reward group generally showed intermediate theta levels during these early blocks; while largely non-significant compared to the other groups, a trend-level difference emerged in Block 2, where the Adaptive group exhibited marginally higher theta power than the Reward group ($p = .072$). However, a shift occurred in the final block as frontal theta power for the Adaptive group ($M = 0.178$, $SEM = 0.005$) dropped to a trend level below both the Control group ($M = 0.208$, $SEM = 0.007$; $p = .071$) and the Reward group ($M = 0.207$, $SEM = 0.005$; $p = .085$), see Fig. 4 and Fig. 5.

A complementary pattern emerged in the parietal alpha band. The Mixed ANOVA revealed no main effect of Group, $F(2, 35) = 0.87$, $p = .428$, $\eta_p^2 = .052$, but a significant main effect of Block, $F(3, 105) = 3.10$, $p = .032$, $\eta_p^2 = .089$. Similar to theta activity, a significant Group by Block interaction was observed, $F(6, 105) = 4.14$, $p = .002$, $\eta_p^2 = .206$. Post-hoc analyses demonstrated that parietal alpha levels remained relatively stable and largely indistinguishable across all three groups during Blocks 1, 2, and 3, though marginal trend-level differences were observed in Blocks 2 and 3, where the Control group exhibited slightly higher alpha power compared to the Reward group ($p = .099$ and $p = .100$, respectively), see Fig. 6.

Table 2
Pairwise Post-Hoc Comparisons for Alpha and Theta band power

ROI	Block	Comparison	Mean Difference	t-value	p-FDR
Frontal Theta	1	Adaptive vs. Control	0.025	2.226	0.038
	1	Adaptive vs. Reward	0.011	1.159	0.266
	1	Control vs. Reward	-0.014	-1.414	0.171
	2	Adaptive vs. Control	0.029	2.507	0.022
	2	Adaptive vs. Reward	0.018	2.003	0.072
	2	Control vs. Reward	-0.011	-1.224	0.236
	3	Adaptive vs. Control	0.022	2.215	0.039
	3	Adaptive vs. Reward	0.009	0.968	0.348
	3	Control vs. Reward	-0.014	-1.479	0.152
	4	Adaptive vs. Control	-0.017	-1.87	0.071
	4	Adaptive vs. Reward	-0.016	-1.92	0.085
	4	Control vs. Reward	0.001	-0.005	0.996
Parietal Alpha	1	Adaptive vs. Control	-0.013	-0.572	0.576
	1	Adaptive vs. Reward	-0.002	-0.142	0.889
	1	Control vs. Reward	0.011	0.459	0.651
	2	Adaptive vs. Control	-0.03	-1.258	0.229
	2	Adaptive vs. Reward	0.014	1.311	0.208
	2	Control vs. Reward	0.045	1.742	0.099
	3	Adaptive vs. Control	-0.038	-1.345	0.2
	3	Adaptive vs. Reward	0.013	1.195	0.248
	3	Control vs. Reward	0.051	1.747	0.099
	4	Adaptive vs. Control	-0.013	-0.531	0.603
	4	Adaptive vs. Reward	0.001	-0.022	0.982
	4	Control vs. Reward	0.012	0.474	0.64

Impact on behaviour

Performance by Group and Block

We hypothesised that performance would differ by Group across learning blocks, with Reward participants performing similarly to Adaptive participants, while better than Control participants. An ART mixed model revealed a significant main effect of learning block on score, F (2, 82) = 101.92, p < .001, η_p^2 = .713. Tukey-corrected pairwise comparisons showed a stepwise increase in performance across all blocks: scores in Block 2 (M = 38.20, SD = 12.70) were significantly lower than Block 3 (M = 47.80, SD = 12.70, p < .001) and Block 4 (M = 51.80, SD = 11.80, p < .001), and Block 3 scores were significantly lower than Block 4 (p < .001), indicating consistent learning across the session. Accuracy improved significantly across learning blocks, indicating robust task learning across the session. However, neither the main effect of Group nor the Group by Block interaction was significant. Thus, the adaptive and reward manipulations did not produce detectable immediate accuracy benefits relative to control under the present task constraints.

Feedback time

Feedback time was analysed with the same mixed-effects structure at the trial level (random intercept for participant). Average and standard deviation feedback time (s) is shown in Fig. 3b. Because Control and Reward participants received a fixed 5s feedback duration throughout, whereas the Adaptive group received dynamically adjusted feedback (3–8 s), block and interaction effects primarily reflected changes in the Adaptive condition. Relative to Block 1, feedback time differed across Blocks 2–4 (Block 2: z = − 1.84, p = .066; Block 3: z = − 22.80, p < .001; Block 4: z = − 32.19, p < .001), and significant group by block interactions indicated that these blockwise changes were specific to the Adaptive group (all interaction zs > 17.5, all ps < .001). A mixed ANOVA on participant Block means showed no main effect of Group, F(2, 33) = 0.17, p = .843, η_p^2 = .01, but a significant main effect of Block, F(3, 99) = 4.51, p = .005, η_p^2 = .12 (Greenhouse–Geisser corrected p = .038), and a significant Group by Block interaction, F(6, 99) = 6.77, p < .001, η_p^2 = .29. The same interaction was obtained when Block means were derived from averages of 16 within-block sub-bins, F(6, 99) = 6.77, p < .001, η_p^2 = .29. In Block 4, one-tailed comparison indicated that the Adaptive group (M = 4.54 s, SD = 1.69) tended toward shorter feedback than Control and Reward (M = 5.01 s, SD < 0.01, p = .087).

Impact on physiological states

We expected physiological measures to differ by Group and Block, with parasympathetic dominance increasing in a stepwise manner (C < R < A). An ART mixed model on ratio HRV revealed a significant main effect of Group, F (2, 30.91) = 4.93, p = .014, η_p^2 = .242, while the main effect of Block and the Block by Group interaction were non-significant. Tukey-corrected pairwise comparisons indicated that ratio HRV differed significantly between Control participants (M = 1.17, SD = 0.46) and Reward participants (M = 0.78, SD = 0.31, p = .048) and between Control participants Adaptive participants (M = 0.76, SD = 0.23, p = .026). In other words, autonomic measures showed group-level differences consistent with lower

physiological strain in the intervention groups relative to control. LF/HF differed by Group, with control showing higher values than reward and adaptive conditions. For phasic EDA, a main effect of Group approached significance, F (2,25.64) = 2.94, p = .071, η_p^2 = .187, with Adaptive participants (M = 0.08, SD = 0.33) showing marginally significantly lower phasic EDA than Reward participants (M = 0.30, SD = 0.16, p = .071). No significant effects of Group or Block by group interaction were found. Given the interpretive complexity of LF/HF and the marginal EDA effect, these results are treated as convergent but not definitive evidence of altered autonomic state.

Impact on perception

Satisfaction and Intention to Recommend

We expected that satisfaction and intention to recommend would differ by Group. Results revealed no effect of Group on intention to recommend. A second Kruskal-Wallis test was performed to identify Group differences in satisfaction scores. The effect of Group was significant significance χ^2 (2) = 7.869, p = .01956, η² = .143, where Reward participants (M = 6.29, SD = 0.73) tended to report higher satisfaction scores than Adaptive participants (M = 4.83, SD = 1.40, p = .025).

Intrinsic Motivation as a Moderator Between Group and Score

To examine whether intrinsic motivation dimensions moderated the relationship between Group and Block 4 performance, four moderation analyses were conducted with Group, IM dimension, and their interaction as predictors. Bonferroni correction was applied to control for multiple comparisons. No significant Group by IM interactions were found after correction (all p-corrected > .05), indicating that group membership did not moderate the relationship between any IM dimension and Block 4 performance. Main effects models were subsequently examined. Only perceived competence significantly predicted Block 4 performance after Bonferroni correction, F (3,40) = 11.57, p < .001, R^2 = .465, adjusted R^2 = .424, such that higher perceived competence was associated with higher performance, β = 5.43, SE = 1.02, t (40) = 5.30, p < .001. Interest and effort did not significantly predict performance after correction. Group membership was not a significant predictor in any model.

Intrinsic Motivation as a Moderator Between Group and Engagement

The same analytic strategy was applied with engagement as the outcome variable. Moderation analyses revealed no significant group motivation interactions after Bonferroni correction (all p-corrected > .05). Main effects models revealed that two IM dimensions significantly predicted engagement after correction. Interest was the strongest predictor, F (3,40) = 25.82, p < .001, R^2 = .659, adjusted R^2 = .6534, with higher interest associated with greater engagement, β = 0.41, SE = 0.05, t (40) = 8.68, p < .001. Additionally, effort significantly predicted engagement, F (3,40) = 6.32, p = .001, R^2 = .322, adjusted R^2 =

.271, where higher effort scores predict higher reported engagement β = 0.34, *SE* = 0.08, *t* (40) = 4.23, *p* < .001. Perceived competence did not survive the Bonferroni correction (*p* = .017). Group membership was not a significant predictor in any model.

Discussion

This study tested whether EEG-based closed-loop feedback pacing could regulate task-load dynamics during digital learning. The main finding is a dissociation between behavioural and neurophysiological outcomes. Accuracy improved across blocks in all groups, with no evidence that neuroadaptive pacing improved immediate performance relative to fixed-feedback control or reward. In contrast, EEG-derived task-load measures showed group-specific trajectories, with the neuroadaptive condition showing reduced task load over time. These findings suggest that adaptive feedback pacing altered neurophysiological state dynamics while preserving learning performance.

Regardless of group membership, learners achieved a high level of performance. However, examining TL, there was a nonlinear effect across learning blocks, highlighting how each group reached similar behavioural destinations through different cortical activations, suggesting different cognitive processes. The control group displayed a compensatory profile. Low frontal theta and high parietal alpha activity throughout much of the task suggest early disengagement or under-stimulation. Furthermore, the control group ended the task with a spike in frontal theta and a drop in parietal alpha, indicating a forced high cognitive demand “catch-up” or compensatory state due to insufficient encoding early on. The reward group displayed a steady profile, maintaining consistent levels of both frontal theta and parietal alpha across all four task blocks. Here, extrinsic motivation acted as a powerful buffer against both early disengagement and late-stage fatigue, maintaining a steady, artificial level of engagement. The adaptive group portrayed efficient learners. High frontal theta and low parietal alpha in the first blocks indicate high early cognitive resource allocation; the system forced efficient early encoding, which successfully consolidated learning gains. Consequently, by the end of the task, a shift to low frontal theta and high parietal alpha suggests that the learners were able to safely release cognitive resources without sacrificing performance.

Across four blocks, all groups improved; the reward group attained greater satisfaction; the adaptive group exhibited selectively lower late-stage TL relative to control, with autonomic indices also favouring both intervention arms over control, through distinct physiological signatures. The practical message is bifurcated: if immediate accuracy and perceived quality are objectives, extrinsic reward is effective; if regulating cognitive strain is the priority, a closed-loop scaffold shows targeted advantages that are neurally coherent. The neuroadaptive system appeared to correctly map to the learner’s cognitive process activation. Encoding time started high (> 5s) when the brain was actively building the mental models and decreased (< 5s) in later blocks as the brain became more efficient. The lack of outright differences in objective performance metrics may not be a failure of the system, but rather an artifact of the experimental boundaries. The task may not have been long enough or difficult enough to induce

severe cognitive overload or mental fatigue that would have penalized performance. In short, the control group matched the adaptive group's accuracy, yet at a higher cognitive price.

Self-reported evaluations showed selective effects. Intention to recommend did not differ by group. Satisfaction favoured Reward over Neuroadaptive, consistent with the immediate, easily interpretable benefit of incentives in a fixed interface. Intrinsic motivation (IM) dimensions played distinct roles. Competence predicted Block 4 scores. Engagement did not differ by group, but it covaried with IM: higher interest and effort each predicted higher engagement. None of the IM dimensions moderated the group by engagement relationship, indicating that the interventions did not directly shift engagement once IM is accounted for.

Differences in autonomic activity, specifically sympathovagal balance and sympathetic reactivity further distinguish Reward from Adaptive. Phasic EDA showed a group effect, where activity was lower in Adaptive compared to Reward. HRV (LF/HF) differed by group as well, with Control exhibiting higher LF/HF than both Reward and Adaptive Interpreted conventionally, Control showed greater sympathetic dominance, while both interventions were associated with a more favourable autonomic balance. Although physiology and TL were not modelled jointly, the pattern is consistent with reduced systemic strain under either motivational incentives or adaptive pacing.

Several limitations constrain interpretation. First, the sample was modest and analytic sample sizes varied across outcomes because of physiological and EEG data-quality constraints. Second, the adaptive policy manipulated feedback duration rather than task difficulty, content complexity, or instructional support. Third, task-load thresholds were group-based rather than individualized, limiting sensitivity to person-specific EEG profiles. Fourth, motivation and engagement were measured only after the task, preventing blockwise analysis of motivational dynamics. Fifth, the study did not include retention or transfer outcomes, so conclusions are limited to immediate learning performance and state regulation. Sixth, the autonomic measures provide convergent but indirect evidence of physiological strain and should not be interpreted as definitive stress markers. Finally, the reward manipulation involved an expectancy procedure in which all participants ultimately received equal draw entries; this should be interpreted as a motivational manipulation rather than a direct monetary-performance contingency.

Holistically, the scalp topography maps provide promising results that merit further investigation. The frontal and parietal areas discussed can be further mapped to the extensively studied Broadman's areas, which would reveal additional, more salient insights into the cognitive mechanisms at work in the neuroadaptive learning task. Research points to Broadman's areas 6, 8, and 39 to be exceptionally involved in working memory, specifically the encoding of semantic and visual information [52, 53]. To offer a more granular investigation, additional analyses could examine neural oscillations based on specific event-related markers, visualizing connectivity through phase transfer entropy [54].Future studies could employ more sophisticated techniques such as functional near-infrared spectroscopy (fNIRS), magnetoencephalography (MEG) or magnetic resonance imaging (MRI) to pinpoint the underlying mechanisms in the areas of interest. The results at hand are promising, showcasing group

differences during a single task. Additional analyses, such as brain connectivity, would be interesting to conduct as a means of determining cortical activation patterns across groups and different tasks.

Several design choices remain open, each pointing to concrete steps to broaden generalizability and impact. (i) Task ecology and horizon. The selective late-block benefits of the Adaptive group suggest compounding gains in longer or more demanding tasks. Extending to longitudinal protocols (days–weeks) and harder materials should test whether state regulation translates into larger accuracy, retention, and transfer effects. (ii) Algorithmic TL estimation. Replace quartile-based thresholds with individualized machine-learning classifiers (e.g., cross-validated, online-updating models) that integrate multiband features and temporal dynamics; this should improve sensitivity and robustness across learners and sessions. (iii) Multimodal sensing. Augment EEG with fNIRS to capture prefrontal hemodynamics related to effort/control. Incorporate pupillometry to obtain a lightweight, commercially feasible proxy for cognitive load; a hybrid EEG+pupil TL index may approach EEG-only fidelity with lower deployment burden. (iv) Advanced EEG analytics. Move beyond bandpower to activity/connectivity measures (e.g., frontal–parietal coherence, aperiodic 1/f slope, source-localized generators) and phase-specific time–frequency decompositions to refine mechanisms and identify responders. (v) Broader physiology. Add respiration and pulse-derived metrics alongside HRV and both tonic and phasic EDA, enabling flexible sensor configurations while maintaining state fidelity. (vi) Outcomes beyond accuracy. Include efficiency (accuracy per unit time), retention/transfer, and metacognitive calibration; adaptive systems that chiefly regulate state may yield their largest benefits in durable learning rather than immediate correctness under fixed constraints. (vii) Adaptive policy space. Expand beyond outcome-time modulation to multi-lever controllers that jointly optimize task difficulty, spacing, and feedback—potentially via constrained reinforcement learning that balances accuracy, TL, and efficiency. (viii) Hardware pragmatics. Test reduced-channel, dry-electrode EEG focused on the TL ROIs and camera-based pupillometry to evaluate performance in realistic, scalable deployments.

Taking into consideration all the indicators of system success, it is evident that, overall, the neuroadaptive system was successful in regulating TL. The system appears to have minimised stress levels, optimised performance requiring less cognitive resources, and benefited from dimensions of intrinsic motivation. Despite the lack of widespread interaction effects between group and learning blocks, learners overall exhibit a more stable cognitive state and an enhanced user experience when using the neuroadaptive system, given significant group differences in neurophysiological indices.

Methods

This study used a randomised, between-subjects experimental design to examine the effects of extrinsic motivation and neuroadaptive support during a learning task. Participants completed a multi-block interactive task while neurophysiological (EEG), physiological, and self-report data were collected. Measures captured cognitive load, autonomic activation, intrinsic motivation, engagement, and user experience. EEG data was pre-processed using a standard protocol. Data were analysed using a

combination of parametric, nonparametric, and mixed-effects statistical approaches appropriate to the distributional properties of the measures.

Participants

Fifty-one adults (24 F; age *M* = 26.61, *SD* = 5.76) participated in the study. The sample size is consistent with prior BCI studies using similar methods requiring intensive data collection (Apicella et al., 2022; Beauchemin et al., 2024; Karran et al., 2019). Participants were recruited from our institution's panel based on good health, normal or corrected vision, no history of neurological disorders, and advanced oral and written French proficiency. Participants were compensated $60 for their participation and entered in a draw for a $200 Visa gift card, in line with the extrinsic motivation condition described in the following section. Ethical approval was obtained from the research ethics board of HEC Montréal (Certificate 2023–5071). The study was conducted in accordance with institutional guidelines and regulations.

Procedure

Participants were randomly assigned to one of three groups: Control (no reward, no adaptivity) (C; *n* = 19), reward and no neuroadaptive countermeasures (R; *n* = 16), neuroadaptive countermeasures and no reward (A; *n* = 16). Data collection sessions, conducted in French, lasted approximately 150 minutes. After providing informed consent and demographic information, participants underwent tool installation and signal verification (EEG impedance check and artefact inspection). Baseline tasks were included to establish reference measurements for physiological and EEG data. Participants completed a pre-task questionnaire to collect demographic information and assess prior knowledge of the task content, followed by four blocks of the learning task. Reward participants were informed they would earn one entry into a $200 prepaid Visa gift card draw for every 10% improvement in their block scores. Post-task questionnaires measured IM and engagement. To preserve ethical parity across conditions, all participants ultimately received the same number of entries. Participants signed a compensation form for electronic payment and were thanked before departure.

Experimental Design

The study used a between-subjects, three-group design where the independent variables were extrinsic motivation and neuroadaptivity. Extrinsic motivation took the form of entries into a draw for a monetary reward, where the more correct responses during the task, the more entries participants believed they would receive. At the end of the study, all participants received the same number of entries in the draw. Gender, level of education, and prior constellation knowledge did not differ between groups. Thus, these variables were not used as covariates in testing the hypotheses.

Measures

Physiological

Regarding physiological measures, heart rate variability (HRV) was calculated as the ratio of low-frequency power (0.04 Hz – 0.15 Hz) over high-frequency power (0.15 Hz – 0.4 Hz) (LF/HF) [55] during each block. Electrodermal activity (EDA) was measured as average phasic EDA across each block, created from data recorded at 250Hz averaged every second [56]. These two physiological measures were used as proxies for autonomic activation [57].

Intrinsic Motivation

To measure IM, we adapted the Intrinsic Motivation Inventory, originally developed by Ryan [58]. The scale consists of 7 subscales, totalling 45 items. Traditionally, each item is rated using a 7-point Likert scale from “not at all true” to “very true”. The scale was shortened to 11 items based on a 2011 study by Sun and Gao with a Cronbach alpha of .92. The current study’s Cronbach’s alpha calculation indicated a level of internal consistency of .69. Therefore, the three dimensions (interest α = .88, effort α = .88, and competence α = .95) were investigated independently.
To measure IM, we adapted the Intrinsic Motivation Inventory, originally developed by Ryan [58]. The scale consists of 7 subscales, totalling 45 items. Traditionally, each item is rated using a 7-point Likert scale from “not at all true” to “very true”. The scale was shortened to 11 items based on a 2011 study by Sun and Gao with a Cronbach alpha of .92. The current study’s Cronbach’s alpha calculation indicated a level of internal consistency of .69. Therefore, the three dimensions (interest α = .88, effort α = .88, and competence α = .95) were investigated independently.

Engagement

Perceived engagement was measured using an engagement scale developed by de Vreede et al. [59]. The scale is composed of three dimensions: affective engagement, behavioural engagement, and cognitive engagement. The scale is composed of 15 items in total. During the creation of the scale, the authors reported a Cronbach’s alpha of .73 for the cognitive factor, .92 for the behavioural factor, and .86 for the affective factor. Initially created to have a discipline-independent definition and measure of engagement, the scale has since been used to assess engagement with artificial intelligence [60]. This study reported similar Cronbach’s alphas for the three factors: .90, .90, and .92, respectively. The scale was reduced to three items per dimension based on the highest factor loadings of the de Vreede et al. [60] study. The current study’s Cronbach’s alpha calculation revealed an acceptable level of internal consistency (α = 0.72); therefore the dimensions were combined.

Intention to recommend and satisfaction

We used the Net Promoter Score (NPS) developed by Reichheld [61] to measure individuals' intention to recommend. The NPS is a single-item scale scored on an 11-point Likert scale, where 0 denotes "not likely" and 10 denotes "likely". To measure satisfaction, we used the Customer Satisfaction Score (CSAT) developed by Faris et al. [62]. It is a single-item scale, scored on a 7-point Likert scale where 1 represents "not satisfied" and 7 represents "satisfied". Prior knowledge was measured with two single-item questions to get a general idea of participants' knowledge of the task content, as well as a 10-item scale adapted from Flynn and Goldsmith [63].

Experimental Stimuli

The interactive user interface was adapted from Riopel et al. [64]. This specific task was chosen as it was anticipated that participants were likely to be unfamiliar with the content. The original task was comprised of 88 constellations. Of these constellations, 32 were selected for this learning task based on shape similarity to increase the task's difficulty. The stimuli were presented in four blocks. Each constellation was shown in conjunction with four possible responses for the participant to select. The interface displayed a countdown below the response options during the response portion and the outcome portion of each trial. Response time was fixed at five seconds. Outcome time was fixed at five seconds for the C and R conditions. The outcome time for the N condition started at five seconds for the first trial, then varied by one second depending on the classified task load. The outcome time could vary between three and eight seconds, inclusively. Each constellation was presented twice per block, in a pre-determined randomized order, giving 64 trials per block.
Perceived engagement was measured using an engagement scale developed by de Vreede et al. [59]. The scale is composed of three dimensions: affective engagement, behavioural engagement, and cognitive engagement. The scale is composed of 15 items in total. During the creation of the scale, the authors reported a Cronbach's alpha of .73 for the cognitive factor, .92 for the behavioural factor, and .86 for the affective factor. Initially created to have a discipline-independent definition and measure of engagement, the scale has since been used to assess engagement with artificial intelligence [60]. This study reported similar Cronbach's alphas for the three factors: .90, .90, and .92, respectively. The scale was reduced to three items per dimension based on the highest factor loadings of the de Vreede et al. [60] study. The current study's Cronbach's alpha calculation revealed an acceptable level of internal consistency ($\alpha = 0.72$); therefore the dimensions were combined.

Intention to recommend and satisfaction

We used the Net Promoter Score (NPS) developed by Reichheld [61] to measure individuals' intention to recommend. The NPS is a single-item scale scored on an 11-point Likert scale, where 0 denotes "not likely" and 10 denotes "likely". To measure satisfaction, we used the Customer Satisfaction Score (CSAT) developed by Faris et al. [62]. It is a single-item scale, scored on a 7-point Likert scale where 1 represents "not satisfied" and 7 represents "satisfied". Prior knowledge was measured with two single-item

questions to get a general idea of participants' knowledge of the task content, as well as a 10-item scale adapted from Flynn and Goldsmith [63].

Experimental Stimuli

The interactive user interface was adapted from Riopel et al. [64]. This specific task was chosen as it was anticipated that participants were likely to be unfamiliar with the content. The original task was comprised of 88 constellations. Of these constellations, 32 were selected for this learning task based on shape similarity to increase the task's difficulty. The stimuli were presented in four blocks. Each constellation was shown in conjunction with four possible responses for the participant to select. The interface displayed a countdown below the response options during the response portion and the outcome portion of each trial. Response time was fixed at five seconds. Outcome time was fixed at five seconds for the C and R conditions. The outcome time for the N condition started at five seconds for the first trial, then varied by one second depending on the classified task load. The outcome time could vary between three and eight seconds, inclusively. Each constellation was presented twice per block, in a pre-determined randomized order, giving 64 trials per block.

Instruments and Lab Setup

Participants were situated in a Faraday cage, equipped with a desk, a Lenovo monitor (1920 x 1080, 59.93 Hz), and a chair with adjustable height. There was a two-way mirror between the experimental room and the observation room, where participants could not see into the observation room. In the observation room, there were three computers and five monitors. There was a switch between two monitors to alternate which screen was displayed to the participant. The moderator communicated with the participant via a microphone and speaker. Data synchronization was possible through a sync box that delivered pulses from the COBALT Bluebox [65, 66] to Tobii Pro Lab every 60 seconds. The pulses could then be converted to UTC timestamps, which allowed for complete synchronization between all data sources.

EEG activity was captured using the g.tec NAUTILUS wireless system (g.tec medical engineering GmbH, Schiedlberg, Austria), specifically using the g.SCARABEO active electrodes (g.tec medical engineering GmbH, Schiedlberg, Austria). A 32-electrode EEG montage was configured based on the 10–10 [67] and 10–20 international system [68], with adjustments made to ensure data were captured in the areas of interest. Eight electrodes were identified as crucial to measure task load (F1-4, CP1, CP5, P1, P5). PO3, PO4, O1, and O2 were remapped to accommodate this electrode selection. A ground electrode was placed at Fz, and a reference electrode was placed on the right earlobe as a common baseline to facilitate noise reduction and EEG signal comparison [69].

EEG signals were recorded and processed in real-time using Simulink, a Matlab-based software (version R2021b, IBM), with a real-time sampling rate of 250Hz. A simplified Simulink model can be found in Fig. 2. All 32 channels were saved as raw EEG signals. Additionally, Data for the eight electrodes of

interest were processed in real-time with Bandpass (0.5Hz-50Hz) and Notch (58Hz-62Hz) filters. A Simulink block was also implemented for band-power extraction for the eight electrodes.

Task load was estimated from the ratio of frontal theta power to parietal alpha power using electrodes F1, F2, F3, F4, CP1, CP5, P1, and P5. Sixteen frontal-parietal theta-alpha ratios were computed once per second. Each ratio was classified as low or high relative to lower and upper thresholds derived from the control group from the present study. A majority vote across the 16 ratios produced a one-second task-load classification. A second majority vote across the previous six one-second classifications produced the final task-load state sent to the interface through lab streaming layer. In the adaptive condition, this final state adjusted feedback duration by one-second increments within a 3 to 8 s range. The control and reward groups received fixed 5 s feedback. The algorithm was fixed before adaptive sessions. Because thresholds were group-based rather than individualized, the classifier should be interpreted as a group-calibrated state-regulation mechanism. We therefore report classifier-derived task-load dynamics as a neurophysiological state outcome rather than as a direct measure of learning performance.

EEG preprocessing and analysis

The raw EEG data for all 32 channels were pre-processed and analysed in Python using *MNE-Python* (v 1.11.0) and *Anaconda* following standard protocol [70]. Continuous EEG was filtered using zero-phase FIR filters: high-pass 0.5 Hz to remove slow drifts, low-pass 30 Hz to limit high-frequency noise, and dual notch filters at 58 and 62 Hz to attenuate 60 Hz line noise and sidebands, as well as FIR with zero-phase application to avoid phase distortions. Bad channels were identified by two complementary methods: (a) detection of bridged electrodes via spatial correlation-based screening, and (b) outlier detection of channel variance, with > 5 SD from the mean. Marked channels were interpolated using spherical-spline interpolation. Data were re-referenced to the average reference after bad-channel interpolation. Ocular and other stereotyped artifacts were reduced or removed using ICA, fit on 1 Hz high-pass–filtered data for component stability [71]. To complement annotation-based rejection, automated rejection using *Autoreject* was used when sufficient epochs were available (*n_interpolate* = 4, *consensus* = 0.1) [72]. Epochs were extracted around feedback phases with durations between 3s and 8s, with a small 0.1s pre-onset margin for stability. Whilst in the case of breaks, a 5s epoch window with 1 s overlap was used. Power spectral density (PSD) was estimated via Welch's method with *fmin* = 0.5 Hz, *fmax* = 45 Hz, *n_fft* = 2×sampling rate, and 50% overlap. Theta (4–8 Hz) and Alpha (8–13 Hz) bandpower was computed by averaging PSD within canonical bands. Bandpower was compared using relative power, which was normalized to a baseline derived from the average of the participants break periods within the session and expressed as 10·*log*10 (Pfeedback/Pbaseline) in dB.

Instrumentation

All measurement scales were administered via Qualtrics (Qualtrics, Provo, UT). Participant sessions were recorded using a Razer Kiyo Pro Ultra 4K Webcam mounted on the participants' monitor. An iPad

Air was used to administer the consent and compensation forms via Qualtrics (Qualtrics, Provo, UT). EDA and ECG activity were recorded using the COBALT-Bluebox system [65]. Two EDA sensors were placed on the participant's non-dominant hand, fixed with a compression glove. We utilized a Lead 2 sensor configuration to measure heart rate, whereby one sensor was placed beneath each collarbone, and a third was placed on the participant's second-to-last rib on the left side.

Statistical Analysis

All statistical analyses were conducted in R Version 4.2.1 and RStudio Version 2023.09.1 [73]. Group differences were assessed based on age, education, and prior knowledge. Age substantially differed between groups (p = .064), therefore outliers were identified and removed using the MAD method with a rejection criterion of 2.5 [74]. Due to data quality, sample size differed between analyses depending on the variable under investigation. Group, Block, and Group by Block interaction effects were tested for blockwise outcomes. Participant was included as a random intercept in trial-level mixed-effects models. Nonparametric or aligned-rank-transform models were used when model assumptions were violated. Multiple comparisons were corrected within each outcome family using FDR, Bonferroni, or Tukey adjustment, as specified. All tests were two-tailed unless a directional contrast was pre-specified. Because sample size differed across measures due to signal quality and missingness, results are interpreted with emphasis on effect sizes rather than statistical significance alone.

Declarations

Data Availability

The datasets used and/or analysed during the current study are available from the corresponding author on reasonable request.

Author Contributions

A.J.K., C.C., P.M.L., and S.S. conceptualized and supervised the study. K.S. and T.R.M. performed the data analyses. K.S., A.J.K., T.R.M., and A.R.S. wrote the manuscript. All authors reviewed and approved the final manuscript.

Additional Information

The authors have no competing interests as defined by Nature Research, or other interests that might be perceived to influence the results and/or discussion reported in this paper.

Funding Declaration

This study was made possible thanks to funding from NSERC (RGPIN-2020-06048, ALLRP 565704 – 21) and SSHRC CGS-M.

References

1. Eurostat Individuals - internet activities. Eurostat (2025). https://doi.org/10.2908/ISOC_CI_AC_I
2. Statistics Canada. Selected online activities by gender, age group and highest certificate, diploma or degree completed. *Government Can.* https://doi.org/10.25318/2210013701-ENG (2023).
3. Hongsuchon, T., Emary, I. M. M. E., Hariguna, T. & Qhal, E. M. A. Assessing the Impact of Online-Learning Effectiveness and Benefits in Knowledge Management, the Antecedent of Online-Learning Strategies and Motivations: An Empirical Study. *Sustainability* 14, (2022).
4. Klašnja-Milićević, A., Vesin, B., Ivanović, M. & Budimac, Z. E-Learning personalization based on hybrid recommendation strategy and learning style identification. *Comput. Educ.* **56**, 885–899 (2011).
5. Tekin, C., Braun, J., Van Der Schaar, M. & eTutor Online learning for personalized education. in *IEEE International Conference on Acoustics, Speech and Signal Processing (ICASSP)* 5545–5549 (IEEE, South Brisbane, Queensland, Australia, 2015). 5545–5549 (IEEE, South Brisbane, Queensland, Australia, 2015). (2015). 10.1109/ICASSP.2015.7179032
6. Chaouachi, M., Jraidi, I., Lajoie, S. P. & Frasson, C. Enhancing the Learning Experience Using Real-Time Cognitive Evaluation. *IJIET* 9, 678–688 (2019).
7. Zander, T. O. & Kothe, C. Towards passive brain–computer interfaces: applying brain–computer interface technology to human–machine systems in general. *J. Neural Eng.* **8**, 025005 (2011).
8. Lebedev, M. A. & Nicolelis, M. A. Brain-machine interfaces: from basic science to neuroprostheses and neurorehabilitation. *Physiol. Rev.* **97**, 767–837 (2017).
9. Aricò, P., Borghini, G., Di Flumeri, G., Sciaraffa, N. & Babiloni, F. Passive BCI beyond the lab: current trends and future directions. *Physiol. Meas.* **39**, 08TR02 (2018).
10. Karran, A. J. et al. Toward a Hybrid Passive BCI for the Modulation of Sustained Attention Using EEG and fNIRS. *Front. Hum. Neurosci.* **13**, 393 (2019).
11. Beauchemin, N. et al. Enhancing learning experiences: EEG-based passive BCI system adapts learning speed to cognitive load in real-time, with motivation as catalyst. *Front. Hum. Neurosci.* **18**, 1416683 (2024).
12. Dehais, F. et al. Monitoring Pilot's Cognitive Fatigue with Engagement Features in Simulated and Actual Flight Conditions Using an Hybrid fNIRS-EEG Passive BCI. in. *IEEE International Conference on Systems, Man, and Cybernetics (SMC)* 544–549 (2018). (2018). 10.1109/SMC.2018.00102
13. Pope, A. T., Bogart, E. H. & Bartolome, D. S. Biocybernetic system evaluates indices of operator engagement in automated task. *Biol. Psychol.* **40**, 187–195 (1995).
14. Borghini, G. et al. Real-time Pilot Crew's Mental Workload and Arousal Assessment During Simulated Flights for Training Evaluation: a Case Study. in. *44th Annual International Conference of the IEEE Engineering in Medicine & Biology Society (EMBC)* 3568–3571 (IEEE, Glasgow, Scotland, United Kingdom, 2022). (2022). 10.1109/EMBC48229.2022.9871893

15. Mark, J. A., Kraft, A. E., Ziegler, M. D. & Ayaz, H. Neuroadaptive Training via fNIRS in Flight Simulators. *Front. Neuroergonomics*. **3**, 820523 (2022).
16. Alguindigue, J., Singh, A., Narayan, A. & Samuel, S. Biosignals Monitoring for Driver Drowsiness Detection Using Deep Neural Networks. *IEEE Access.* **12**, 93075–93086 (2024).
17. Liu, Y. T., Lin, Y. Y., Wu, S. L., Chuang, C. H. & Lin, C. T. Brain dynamics in predicting driving fatigue using a recurrent self-evolving fuzzy neural network. *IEEE Trans. neural networks Learn. Syst.* **27**, 347–360 (2015).
18. Sethi, C., Dabas, H., Dua, C., Dalawat, M. & Sethia, D. EEG-based attention feedback to improve focus in E-learning. in *Proceedings of the 2nd international conference on computer science and artificial intelligence* 321–326 (2018). 321–326 (2018). (2018).
19. Gao, X., Lin, H., Wu, X. & Zhang, D. Integrating active brain-computer interfaces (aBCIs) with passive BCIs (pBCIs) under different frustration levels. *Sci. Rep.* **16**, 599 (2025).
20. Spapé, M., Ahmed, I., Harjunen, V. & Jacucci, G. Ravaja, N. A neuroadaptive interface shows intentional control alters the experience of time. *Sci. Rep.* **15**, 9495 (2025).
21. Serrhini, M. & Dargham, A. Toward Incorporating Bio-signals in Online Education Case of Assessing Student Attention with BCI. in Europe and MENA Cooperation Advances in Information and Communication Technologies (eds (eds Rocha, Á., Serrhini, M. & Felgueiras, C.) vol. 520 135–146 (Springer International Publishing, Cham, (2017).
22. Apicella, A. et al. EEG-based measurement system for monitoring student engagement in learning 4.0. *Sci Rep* **12**, (2022).
23. Parsons, B. & Faubert, J. Enhancing learning in a perceptual-cognitive training paradigm using EEG-neurofeedback. *Sci. Rep.* **11**, 4061 (2021).
24. Vygotsky, L. S. & Cole, M. *Mind in Society: Development of Higher Psychological Processes* (Harvard University Press, 1978).
25. Zheng, J., Lajoie, S. P., Wang, T. & Li, S. Supporting self-regulated learning in clinical problem-solving with a computer-based learning environment: the effectiveness of scaffolds. *Metacognition Learn.* **18**, 693–709 (2023).
26. VanLehn, K. The relative effectiveness of human tutoring, intelligent tutoring systems, and other tutoring systems. *Educational Psychol.* **46**, 197–221 (2011).
27. Azevedo, R. & Hadwin, A. F. Scaffolding self-regulated learning and metacognition–Implications for the design of computer-based scaffolds. *Instr. Sci.* **33**, 367–379 (2005).
28. Belland, B. R., Walker, A. E. & Kim, N. J. A Bayesian network meta-analysis to synthesize the influence of contexts of scaffolding use on cognitive outcomes in STEM education. *Rev. Educ. Res.* **87**, 1042–1081 (2017).
29. Quintana, C. et al. Psychology Press,. A scaffolding design framework for software to support science inquiry. in *Scaffolding* 337–386 (2018).

30. Paas, F., Renkl, A. & Sweller, J. Cognitive Load Theory and Instructional Design: Recent Developments. *Educational Psychol.* **38**, 1–4 (2003).
31. Sweller, J. Element Interactivity and Intrinsic, Extraneous, and Germane Cognitive Load. *Educ. Psychol. Rev.* **22**, 123–138 (2010).
32. Hart, S. G. & Staveland, L. E. Development of NASA-TLX (Task Load Index): Results of Empirical and Theoretical Research. in *Advances in Psychology* vol. 52 139–183 (Elsevier, 1988).
33. Wickens, C. D. Multiple Resources and Mental Workload. *Hum. Factors*. **50**, 449–455 (2008).
34. Karran, A. J. et al. Assessing Task Load using Functional Near-Infrared Spectroscopy. in *Proceedings of the NeuroIS Retreat 2026* 212–219 (2026).
35. Feldon, D. F., Callan, G., Juth, S. & Jeong, S. Cognitive load as motivational cost. *Educational Psychol. Rev.* **31**, 319–337 (2019).
36. Gevins, A., Smith, M. E., McEvoy, L. & Yu, D. High-resolution EEG mapping of cortical activation related to working memory: effects of task difficulty, type of processing, and practice. *Cerebral cortex (New York, NY:)* 7, 374–385 (1997).) 7, 374–385 (1997). (1991).
37. Klimesch, W. EEG alpha and theta oscillations reflect cognitive and memory performance: a review and analysis. *Brain Res. Rev.* **29**, 169–195 (1999).
38. Xie, J. et al. Effects of Mental Load and Fatigue on Steady-State Evoked Potential Based Brain Computer Interface Tasks: A Comparison of Periodic Flickering and Motion-Reversal Based Visual Attention. *PLoS ONE*. **11**, e0163426 (2016).
39. Klimesch, W., Sauseng, P. & Hanslmayr, S. EEG alpha oscillations: the inhibition–timing hypothesis. *Brain Res. Rev.* **53**, 63–88 (2007).
40. Klimesch, W. EEG-alpha rhythms and memory processes. *Int. J. Psychophysiol.* **26**, 319–340 (1997).
41. Borghini, G., Astolfi, L., Vecchiato, G., Mattia, D. & Babiloni, F. Measuring neurophysiological signals in aircraft pilots and car drivers for the assessment of mental workload, fatigue and drowsiness. *Neurosci. Biobehavioral Reviews*. **44**, 58–75 (2014).
42. De Jong, T. Cognitive load theory, educational research, and instructional design: Some food for thought. *Instr. Sci.* **38**, 105–134 (2010).
43. Deci, E. L. & Ryan, R. M. *Intrinsic Motivation and Self-Determination in Human Behavior* (Springer US, 1985). 10.1007/978-1-4899-2271-7Boston, MA.
44. Evans, P., Vansteenkiste, M., Parker, P., Kingsford-Smith, A. & Zhou, S. Cognitive Load Theory and Its Relationships with Motivation: a Self-Determination Theory Perspective. *Educ. Psychol. Rev.* **36**, 7 (2024).
45. Inzlicht, M., Shenhav, A. & Olivola, C. Y. The Effort Paradox: Effort Is Both Costly and Valued. *Trends Cogn. Sci.* **22**, 337–349 (2018).
46. Duan, H., Fernández, G., Van Dongen, E. & Kohn, N. The effect of intrinsic and extrinsic motivation on memory formation: insight from behavioral and imaging study. *Brain Struct. Funct.* **225**, 1561–1574 (2020).

47. Zhozhikashvili, N. et al. Working memory processes and intrinsic motivation: An EEG study. *Int. J. Psychophysiol.* **201**, 112355 (2024).
48. Gruber, M. J., Watrous, A. J., Ekstrom, A. D., Ranganath, C. & Otten, L. J. Expected reward modulates encoding-related theta activity before an event. *NeuroImage* **64**, 68–74 (2013).
49. Pu, M. & Yu, R. Post-encoding frontal theta activity predicts incidental memory in the reward context. *Neurobiol. Learn. Mem.* **158**, 14–23 (2019).
50. Kawasaki, M. & Yamaguchi, Y. Frontal theta and beta synchronizations for monetary reward increase visual working memory capacity. *Soc. Cognit. Affect. Neurosci.* **8**, 523–530 (2013).
51. Brehm, J. W. & Self, E. A. The intensity of motivation. (1989).
52. Kapur, S. et al. The neural correlates of intentional learning of verbal materials: A PET study in humans. *Cogn. Brain. Res.* **4**, 243–249 (1996).
53. Medendorp, W. P. et al. Oscillatory Activity in Human Parietal and Occipital Cortex Shows Hemispheric Lateralization and Memory Effects in a Delayed Double-Step Saccade Task. *Cereb. Cortex*. **17**, 2364–2374 (2007).
54. Lobier, M., Siebenhühner, F., Palva, S. & Palva, J. M. Phase transfer entropy: A novel phase-based measure for directed connectivity in networks coupled by oscillatory interactions. *NeuroImage* **85**, 853–872 (2014).
55. Pagani, M. et al. Power spectral analysis of heart rate and arterial pressure variabilities as a marker of sympatho-vagal interaction in man and conscious dog. *Circul. Res.* **59**, 178–193 (1986).
56. Benedek, M. & Kaernbach, C. A continuous measure of phasic electrodermal activity. *J. Neurosci. Methods*. **190**, 80–91 (2010).
57. Ghiasi, S., Greco, A., Barbieri, R., Scilingo, E. P. & Valenza, G. Assessing Autonomic Function from Electrodermal Activity and Heart Rate Variability During Cold-Pressor Test and Emotional Challenge. *Sci. Rep.* **10**, 5406 (2020).
58. Ryan, R. M. Control and Information in the Intrapersonal Sphere: An Extension of Cognitive Evaluation Theory. *J. Personal. Soc. Psychol.* **43**, 450–461 (1982).
59. de Vreede, T. et al. What is Engagement and How Do We Measure It? Toward a Domain Independent Definition and Scale. in 749–758 (2019).
60. de Vreede, T., Singh, V. K., De Vreede, G. J. & Spector, P. The Effect of AI Engagement on Generative AI Adoption. in 168–176 (2024).
61. Reichheld, F. F. The One Number You Need to Grow. *Harvard Business Rev.* **81**, 46–55 (2003).
62. Farris, P. W., Bendle, N. T., Pfeifer, P. E. & Reibstein, D. J. *Marketing Metrics: The Definitive Guide to Measuring Marketing Performance* (Wharton School Pub., 2010).
63. Flynn, L. R., Goldsmith, R. E. A. & Short Reliable Measure of Subjective Knowledge. *J. Bus. Res.* **46**, 57–66 (1999).
64. Riopel, M. et al. USING INVARIANCE TO MODEL PRACTICE, FORGETTING, AND SPACING EFFECTS. 4334–4341 (Barcelona, Spain, doi:10.21125/edulearn.2017.1935. (2017).

65. Courtemanche, F., Sénécal, S., Fredette, M. & Léger, P. M. COBALT-Bluebox: Multimodal user data wireless synchronization and acquisition system. (2022).
66. Léger, P. M. et al. Caption and Observation Based on the Algorithm for Triangulation (COBALT): Preliminary Results from a Beta Trial. in Information Systems and Neuroscience (ed (ed Davis, F. D.) vol. 58 229–235 (Springer International Publishing, Cham, (2022).
67. Chatrian, G. E., Lettich, E. & Nelson, P. L. Ten Percent Electrode System for Topographic Studies of Spontaneous and Evoked EEG Activities. *Am. J. EEG Technol.* **25**, 83–92 (1985).
68. Klem, G. H., Lüders, H. O., Jasper, H. H. & Elger, C. The ten-twenty electrode system of the International Federation. The International Federation of Clinical Neurophysiology. *Electroencephalogr. Clin. Neurophysiol. Suppl.* **52**, 3–6 (1999).
69. Nunez, P. L. et al. EEG coherency: I: statistics, reference electrode, volume conduction, Laplacians, cortical imaging, and interpretation at multiple scales. *Electroencephalogr. Clin. Neurophysiol.* **103**, 499–515 (1997).
70. Gramfort, A. MEG and EEG data analysis with MNE-Python. *Front Neurosci* **7**, (2013).
71. Frank, G., Makeig, S. & Delorme, A. A. Framework to Evaluate Independent Component Analysis applied to EEG signal: testing on the Picard algorithm. in *IEEE International Conference on Bioinformatics and Biomedicine (BIBM)* 2009–2016 (IEEE, Las Vegas, NV, USA, 2022). 2009–2016 (IEEE, Las Vegas, NV, USA, 2022). (2022). 10.1109/BIBM55620.2022.9994862
72. Jas, M. et al. Automated artifact rejection for MEG and EEG data. *NeuroImage* **159**, 417–429 (2017).
73. R Core Team. *R: A Language and Environment for Statistical Computing* (R Foundation for Statistical Computing, 2022).
74. Leys, C., Ley, C., Klein, O., Bernard, P. & Licata, L. Detecting outliers: Do not use standard deviation around the mean, use absolute deviation around the median. *J. Exp. Soc. Psychol.* **49**, 764–766 (2013).

Figures

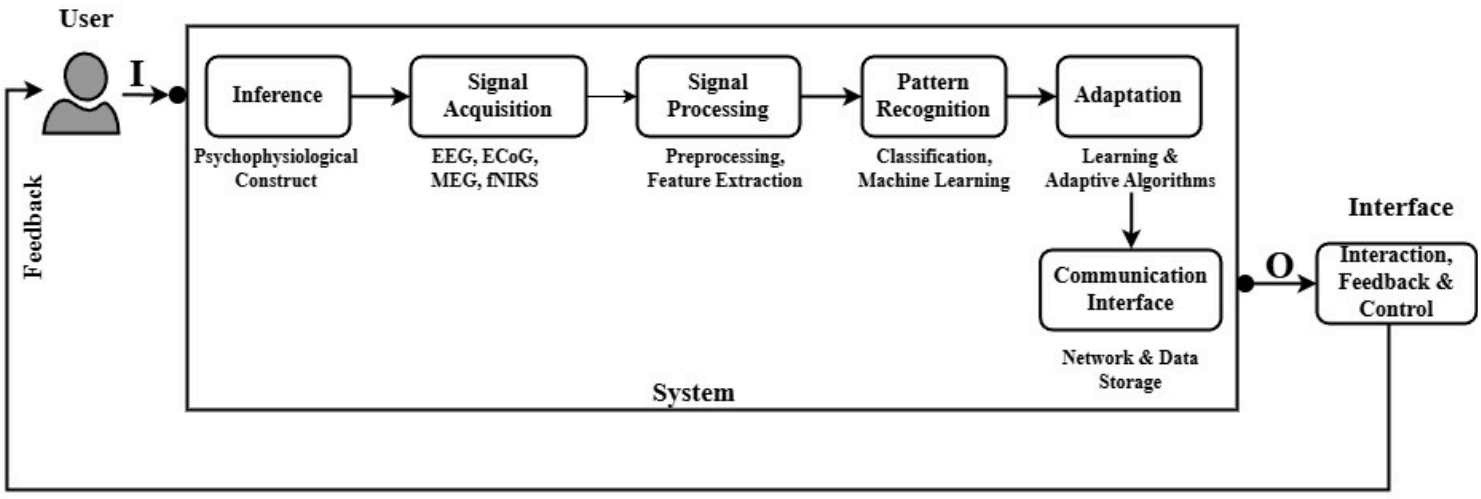


Figure 1

Neurophysiological signals are continuously acquired from the learner using non-invasive sensing modalities such as electroencephalography or functional near-infrared spectroscopy. Extracted features are processed by classification algorithms to infer momentary cognitive states. These inferred states are mapped to predefined adaptation rules that modify system parameters in real time, forming a closed loop between the learner and the digital learning interface.

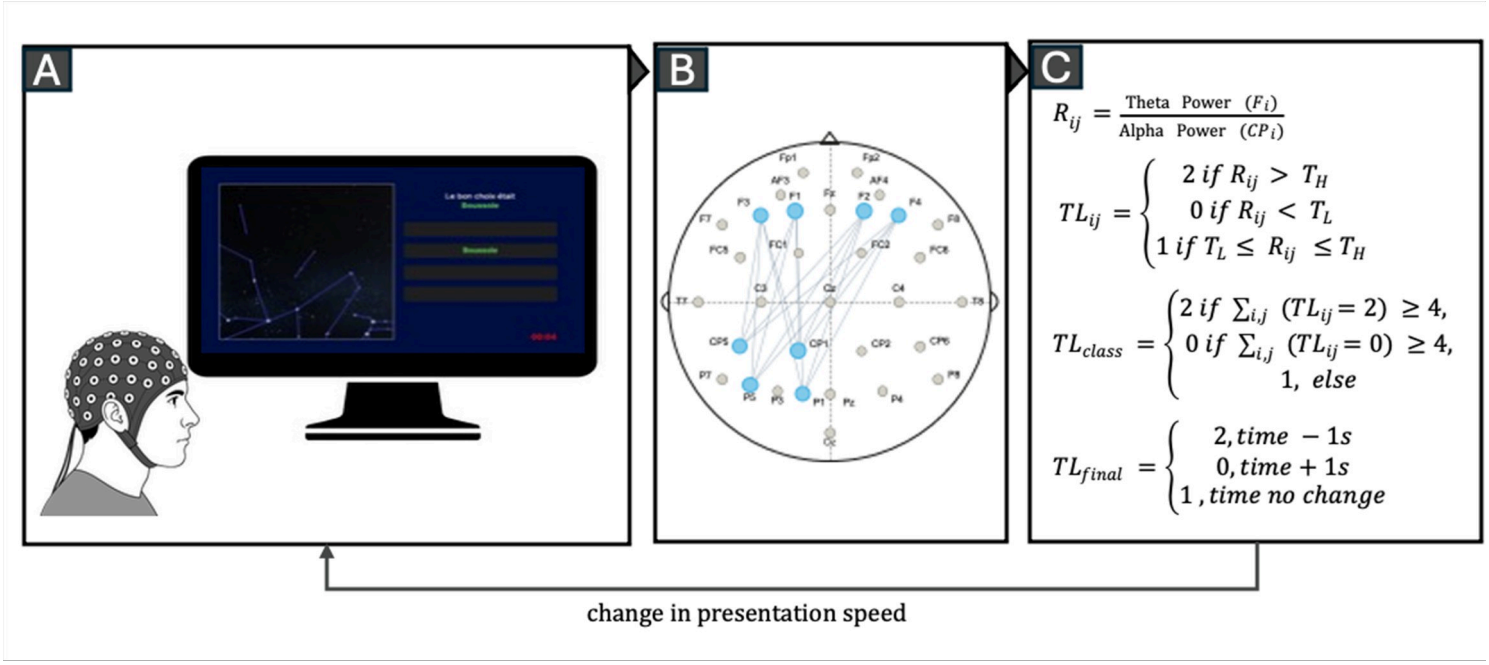


Figure 2

Neuroadaptive Architecture A. Participant encodes correct constellation name. B. EEG montage with visualization of channel pairings. C. Task load (TL) is calculated as a ratio (R) of frontal theta and parietal alpha from 8 electrodes, where i ∈ (F1, F2, F3, F4) and j ∈ (CP1, CP5, P1, P5). High (H) and low (L) thresholds (T) are based on the average ratios at the 1st and 3rd quartiles of the control group. The TL classification (TLclass) (low, medium, high) triggers a change in the stimulus presentation speed (TLfinal).

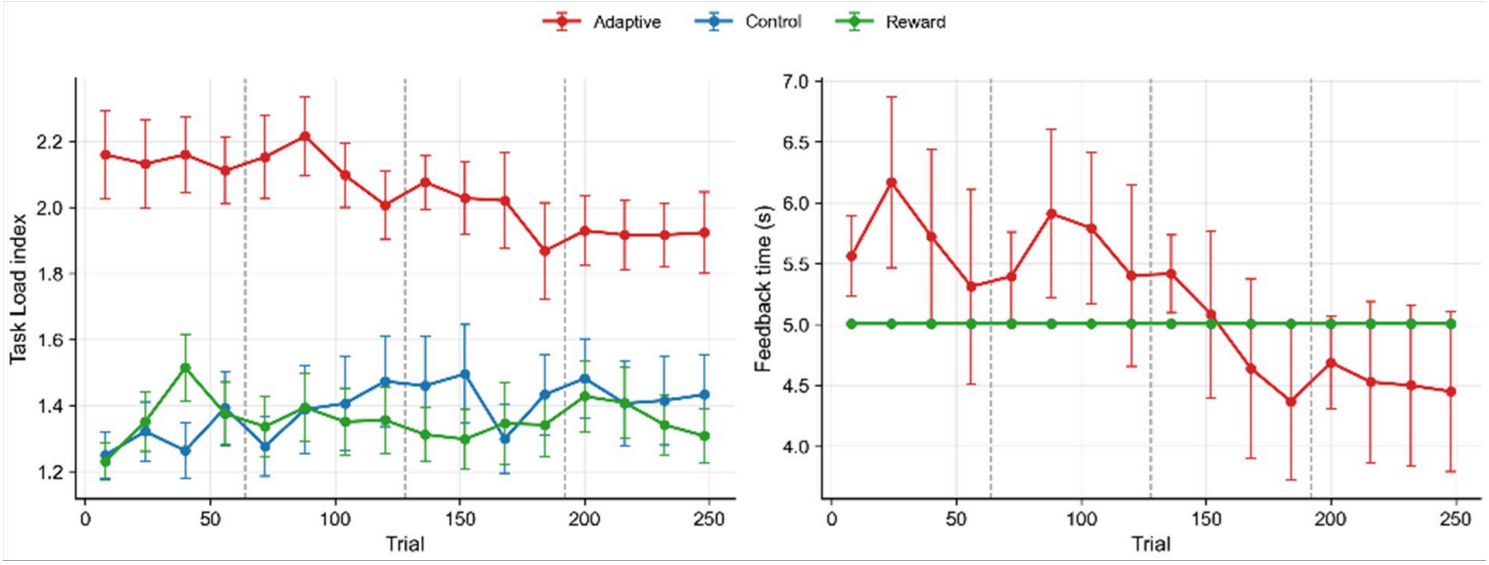


Figure 3

(a) Task Load Index over time per group and block (grey dashed lines). (b) Feedback time per time and block

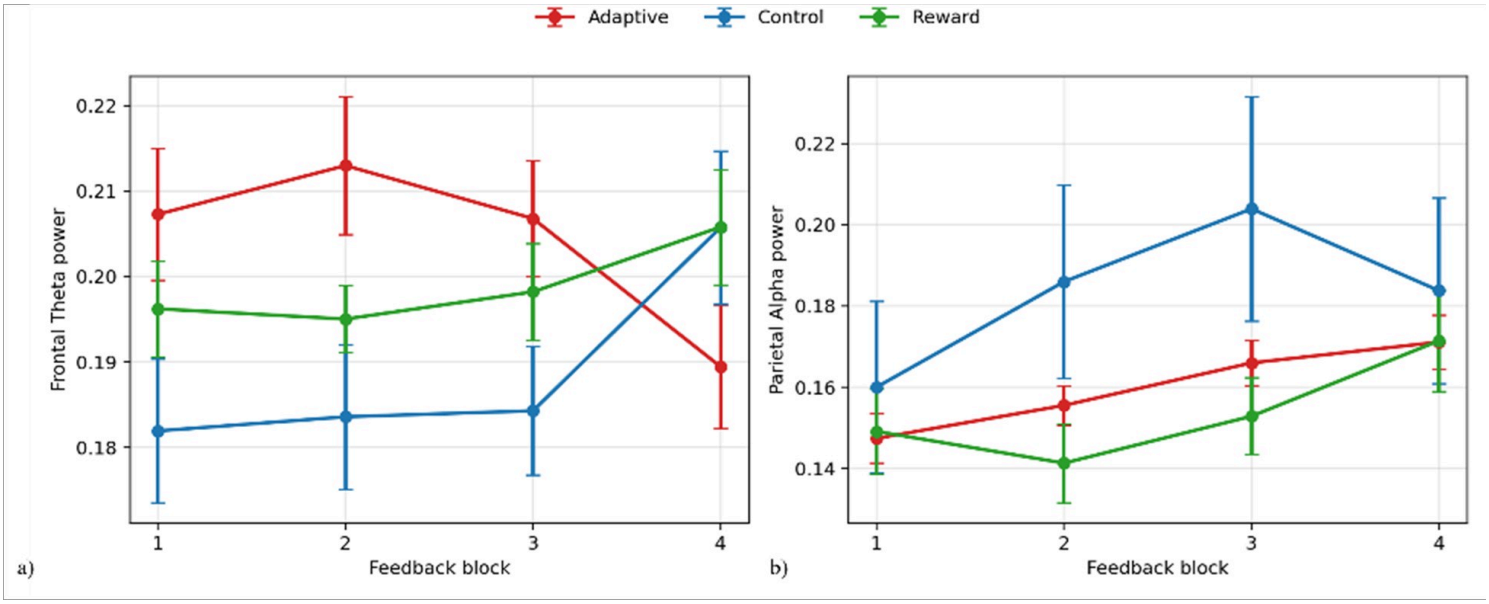


Figure 4

Trajectory of relative power of frontal theta (a) and parietal alpha (b) across the four learning blocks.

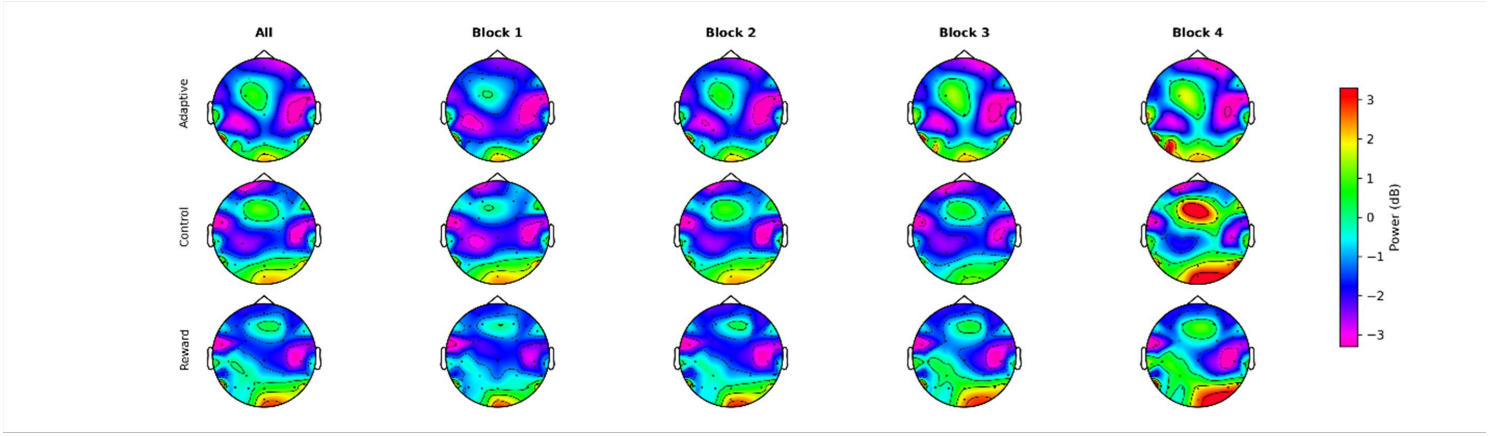


Figure 5

Topographical distribution of relative Theta band power during feedback blocks.

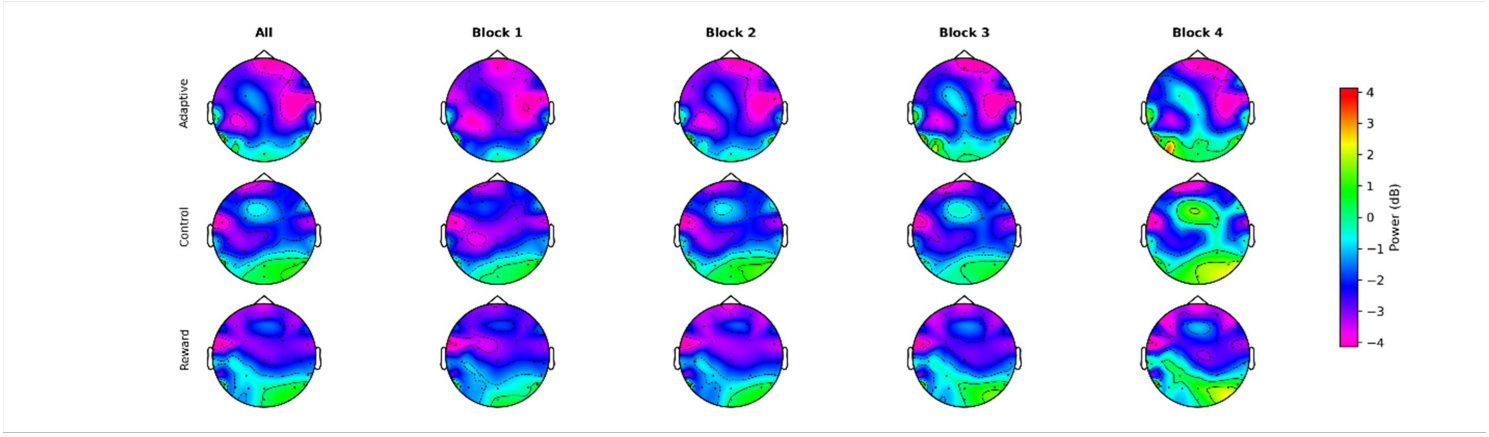


Figure 6

Topographical distribution of relative Alpha band power during feedback blocks.